Tritium removal from JET-ILW after T and D–T experimental campaigns

D Matveev, D Douai, T Wauters, A Widdowson, I Jepu, M Maslov, S Brezinsek, T Dittmar, I Monakhov, P Jacquet, et al.

Tritium removal from JET-ILW after T and D-T experimental campaigns

D. Matveev[a,*], D. Douai[b], T. Wauters[c], A. Widdowson[d], I. Jepu[d], M. Maslov[d], S. Brezinsek[a], T. Dittmar[a], I. Monakhov[d], P. Jacquet[d], P. Dumortier[e], H. Sheikh[d], R. Felton[d], C. Lowry[d], D. Ciric[d], J. Banks[d], R. Buckingham[d], H. Weisen[f], L. Laguardia[g], G. Gervasini[g], E. De La Cal[h], E. Delabie[i], Z . Ghani[d], J. Gaspar[j], J. Romazanov[a], M. Groth[k], H. Kumpulainen[k], J. Karhunen[k], S. Knipe[d], S. Aleiferis[d], T. Loarer[b], A. Meigs[d], C. Noble[d], G. Papadopoulos[d], E. Pawelec[l], S. Romanelli[d], S. Silburn[d], E. Joffrin[b], E. Tsitrone[b], F. Rimini[d], C.F. Maggi[d], and JET Contributors**

[a]Forschungszentrum Juelich GmbH, EURATOM Association, 52425 Jülich, Germany
[b]CEA Cadarache, IRFM, F-13108 Saint Paul Lez Durance, France
[c]ITER Organization, Route de Vinon-sur-Verdon, CS 90 046, F-13067 St Paul Lez Durance Cedex, France
[d]UK Atomic Energy Authority, Culham Science Centre, Abingdon, OX14 3DB Oxfordshire, UK
[e]Laboratory for Plasma Physics, Koninklijke Militaire School - Ecole Royale Militaire, Renaissancelaan 30 Avenue de la Renaissance, B-1000 Brussels, Belgium
[f]Swiss Plasma Center, Station 13, EPFL, 1015 Lausanne, Switzerland
[g]Istituto per la Scienza e Tecnologia dei Plasmi, Consiglio Nazionale delle Ricerche, Bari-Milano, Italy
[h]Fusion National Laboratory, CIEMAT, 28040, Madrid, Spain
[i]Oak Ridge National Laboratory, Oak Ridge, TN 37831-6169, United States of America
[j]Aix-Marseille University, CNRS, IUSTI, Marseille F-13013, France
[k]Aalto University, Department of Applied Physics, 02150 Espoo, Finland
[l]University of Opole, Institute of Physics, Oleska 48, Opole, Poland
***See the author list of J. Mailloux et al, Nucl. Fusion 62, 042026 (2022)*

**Corresponding author: d.matveev@fz-juelich.de*

Abstract

After the second deuterium-tritium campaign (DTE2) in the JET tokamak with the ITER-Like Wall (ILW) and full tritium campaigns that preceded and followed after the DTE2, a sequence of fuel recovery methods was applied to promote tritium removal from wall components. The sequence started with several days of baking of the main chamber walls at 240 ºC and at 320 ºC. Subsequently, baking was superimposed with ion-cyclotron wall conditioning (ICWC) and glow discharge conditioning (GDC) cleaning cycles in deuterium. Diverted plasma operation in deuterium with different strike point configurations, including a raised inner strike point (RISP) configuration, and with different plasma heating – Ion Cyclotron Resonance Frequency (ICRF) and Neutral Beam Injection (NBI) – concluded the cleaning sequence. Tritium content in plasma and in the pumped gas was monitored throughout the experiment. The applied fuel recovery methods allowed reducing the residual tritium content in deuterium NBI-heated plasmas to about 0.1% as deduced from neutron rate measurements. This value is well below the requirement of 1% set by the maximum 14 MeV fusion neutron budget allocated in the ensuing deuterium plasma campaign. The quantified tritium removal over the course of the experiment was $(13.4 \pm 0.7) \cdot 10^{22}$ atoms or (0.67 ± 0.03) g with ~58% attributed to baking, ~12.5% to ICWC, ~26% to GDC, and ~3.5% to first low power RISP plasmas. The experimentally estimated amount of removed tritium is in good agreement with long-term tritium accounting by the JET tritium reprocessing plant, in which the unaccounted amount was reduced by 0.71 g after the cleaning experiment.

1. Introduction

Since 2011, the JET tokamak is equipped with the ITER-Like Wall (ILW) consisting of tungsten (W) and W-coated plasma-facing components (PFC) in the divertor and beryllium (Be) PFC in the main chamber [1]. The most recent achievement at JET-ILW is the second deuterium-tritium (D-T) experimental campaign DTE2 [2] (after DTE1 in 1997 [3]), in which the compatibility of the ITER material mix with high fusion power plasma operation was demonstrated [2]. Tritium accounting, fuel retention and isotope removal are among fundamental scientific and technological questions addressed

by both, DTE1 and DTE2. The DTE2 campaign was preceded and followed by full T campaigns. The total amount of tritium injected into the torus during DTE2 and both T campaigns was $5.04 \cdot 10^{25}$ atoms or 252 g, from which 17 g were introduced via the Neutral Beam Injection (NBI). For comparison, in the DTE1 in total 35 g were injected, of which 0.6 g via NBI [4, 5].

A set of different techniques was applied to help detritiate the torus after the DT and T campaigns. The two main aims were a) to reduce the plasma tritium fraction in the ensuing D campaign below 1% to allow for subsequent D operation in compliance with the allocated 14 MeV neutron budget; and b) to inform ITER on T removal techniques and T retention issues in a tokamak with Be/W wall. The 14 MeV neutron budget for the DTE2 and "isotope" campaigns (i.e. T and subsequent D clean-up campaigns) has been estimated as $1.55 \cdot 10^{21}$ and 10^{20}, respectively [6]. In particular, for the T removal campaign after DT and TT operation, the budget was $5 \cdot 10^{19}$, covering the need for the operation of several tens of high power (40 MW) 5 s long pulses, as well as hundreds of low power pulses.

In the case of DTE1, when JET was operated with a carbon wall, the initial T inventory accumulation rate was found to be about 40% of the injected amount of 35 g [4, 5]. Tokamak plasmas with deuterium fueling reduced the plasma tritium fraction below 1% after few days of operation, while the total inventory leveled off at about 17% of the total input, corresponding to ~6 g of tritium, attributed largely to co-deposited hydrocarbon films and flaked-off co-deposited layers in the divertor [5]. These observations are in agreement with the appraisal of D retention in "all-carbon" JET after the 1985 – 1989 campaigns that was evaluated to be on average 40% of the injected amount, being dominated by co-deposition [7], and with results of the 1993 – 1995 DT campaigns in TFTR with reported average short-term retention of $52 \pm 15\%$ [8, 9]. This experience from tokamaks and subsequent related laboratory and modelling studies reviewed in [10] and [11] resulted in the decision to abandon carbon in the initial material choice for ITER, which was supported by the operation of JET with Be/W wall (JET-ILW) that demonstrated more than factor 10 lower retention rates compared to earlier carbon-wall reference pulses [12].

Prior to DTE2, a full T campaign (both, T gas and T NBI fueling) was executed in JET-ILW in 2021, in particular to clarify isotope effects on energy and particle transport, including the L-H transition. To avoid undesired high D-T neutron rates during the T campaign, a clean-up sequence for D recovery has been developed and applied that essentially implied a two-step isotope-changeover, first from D to H and then from H to T. The D→H changeover comprised baking of the main chamber wall at 320 °C combined with glow discharge conditioning (GDC) and ion cyclotron wall conditioning (ICWC) cycles, followed by tokamak plasma operation at the normal main chamber operation temperature of 200 °C in different magnetic configurations, including one with the raised inner strike point (RISP) [13]. While baking, GDC and ICWC mainly targeted the main chamber wall retention, the RISP plasma configuration was designed to provide increased particle and heat loads to the upper part of the inner divertor (Tile 1, Figure 1a). Indeed, the highest co-deposition of fuel with Be eroded from the main chamber limiters was measured post-mortem in this location after the preceding JET-ILW campaigns, contributing about 50% to the total long-term fuel inventory [14]. It was demonstrated by measurements and modelling that an increase of the surface temperature up to at least 800 °C is needed to achieve a significant fuel release from such co-deposits, especially for experimentally observed layer thicknesses above 10 μm [15-17]. The successful D→H changeover reported in detail in [13] led to a reduction of the plasma deuterium content (in reference diverted plasma pulses in H) to the level of about 1% as required for the subsequent T operation. This experiment laid the basis for the tritium recovery and clean-up strategy to be followed after the T and D-T campaigns. The overall cleaning strategy is described in Section 2 of this contribution. Section 3 and Section 4 are devoted to the detailed analysis of tritium outgassing and removal, whereas implications for ITER drawn from the T removal experience in JET-ILW are discussed in Section 5.

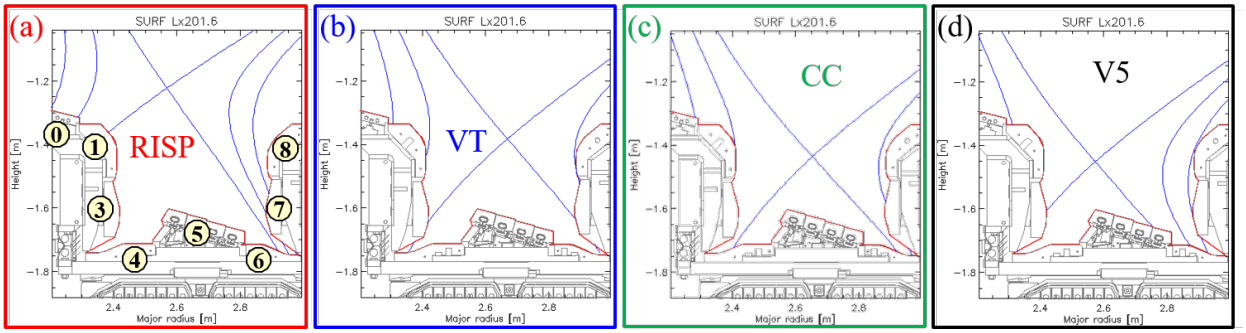

Figure 1. Diverted plasma configurations exploited in JET. Magnetic flux surfaces indicating the inner and outer strike points' positions are shown for the (a) Raised Inner Strike Point (RISP), (b) Vertical Target (VT), (c) Corner-Corner (CC), and (d) Tile 5 (V5) configurations. Conventional numbering of divertor tiles is given for clarity in figure (a).

2. Experimental strategy

Based on the earlier D→H changeover [13], the experimental sequence was designed to benefit from the complementarity of different techniques (baking, ICWC, GDC, diverted plasma pulses). The sequence aims at gradual reduction of the amount of fuel that could be released in discharges, moving from low density low power to high density high power pulses. In this way, the initial baking phase aims at removing the most mobile or weakly bound tritium population from the main chamber walls, reducing the potentially accessible reservoir for ICWC and GDC. Although divertor surfaces remained at lower temperatures during baking (50 °C – 200 °C [13]), the cooling water flow being maintained to protect the in-vessel divertor coils, passive outgassing also plays a role in reducing the T content in the divertor. As the gas release by outgassing/baking follows (empirically) a power law decay with time, fuel removal by baking becomes less efficient after few days of baking at constant temperature. Applying afterwards ICWC pulsing in the presence of the magnetic field (plasma interaction with limiter surfaces) and GDC operation in the absence of the magnetic field (more uniform plasma interaction with recessed areas in the main chamber), both being operated at the baking temperature, promotes additional tritium removal. These primary measures help to reduce the wall T content and related T release during subsequent divertor plasma operation. Diverted plasmas are operated then at first with low power Ion Cyclotron Resonance Frequency (ICRF) heating in different divertor configurations (Figure 1) to ensure low tritium isotopic fraction in plasma. As the T removal sequence could be pursued with high D-NBI power that was not available for the D→H changeover [13] in H (NBI system was not converted to H in that campaign), plasmas with additional auxiliary heating were planned for further divertor cleaning, once the T/(D+T) isotopic ratio reached the level of ~1%, required by the 14 MeV neutron budget allocated to this D plasma phase.

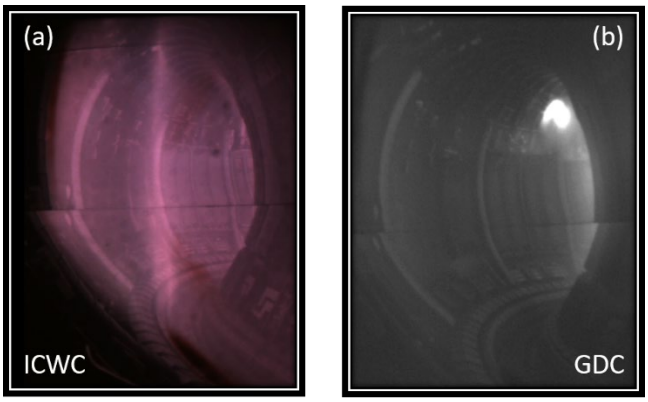

Figure 2. Tangential camera images of a D_2-ICWC (JPN#100288) (a) and typical GDC (b) discharges in JET.

ICWC discharges are produced in JET using the ICRF heating system in the presence of the toroidal magnetic field [18]. RF antennas are operated in monopole phasing in order to maximize coupling to the low density (typically 10^{17} – 10^{18} m^{-3}) ICWC plasmas. For T removal, 18 s long D_2-fed ICWC discharges with 250 – 300 kW of coupled RF power at 29 MHz with a toroidal magnetic field of 1.9 T were used, corresponding to the 2nd harmonic ion cyclotron resonance frequency for D^+ ions, with on-axis resonance layer. A "Barrel-shape" poloidal field of typically 15 mT on-axis is applied to maximize wetted areas by ICWC plasmas, the highest particle fluxes being onto the main chamber surfaces, with parallel ion (D_2^+ and D^+) fluxes up to 10^{21} m^2/s, as well as isotropic CX neutral (D^0) flux about 10^{19} m^2/s. The ion flux to the divertor is, however, much lower ($<10^{16}$ m^2/s), as evidenced in previous attempts to measure it there with Langmuir probes. The D_2 gas is injected with feedback on the torus pressure at ~5×10^{-5} mbar. A tangential camera image of a D_2 ICWC discharge is shown in Figure 2a.

GDC is operated in JET with up to 4 anodes at 2.5 – 4 A and 350 – 400 V, delivering 3 – 3.5 kW of DC power to the plasma, without magnetic field, at a steady D_2 gas flow rate of about 10 mbar-l/s resulting in a stable torus pressure of ~5×10^{-3} mbar [19]. A tangential camera view of a D_2 GDC is shown in Figure 2b. The relatively small surface area of the JET anodes at the top of the vessel, compared to the inner area of the torus, leads to the formation of an anode glow – the bright zone in Figure 2b – affecting the plasma uniformity. However, the D_2^+ ion flux onto both, inner and outer, main chamber JET wall surfaces proved to be fairly uniform, with values of typically 10^{17} m^2/s [20]. As for ICWC, a much lower flux is expected to divertor areas.

Several limitations imposed by the JET Active Gas Handling System (AGHS [21]) had to be taken into account when planning tritium removal. While for the D→H changeover it was possible to perform a gas chromatography analysis of the collected pumped gas by AGHS on a daily basis, namely for ICWC and diverted plasma sessions, such analysis was not possible after T and D-T operations as the system was occupied with T reprocessing and accounting. For this reason, an alternative procedure for daily T accounting has been developed and qualified prior to the T removal sequence. It consists of the Pressure-Volume-Temperature and Residual Gas Analysis (RGA-PVT) of the gas released by the regeneration of the divertor cryogenic pumps into the isolated torus (except for sub-divertor neutral gas diagnostics [22] needed for gas monitoring) after a day of plasma operation with divertor cryogenic pumping only [23]. In such setup, the torus pressure rise upon regeneration of the divertor cryopanels gives the total amount of the released gas (PVT) and RGA with Quadrupole Mass Spectrometry (QMS) systems [22] is used to evaluate the isotopic gas composition. Injections of controlled amounts of D_2 gas into the static torus containing the regenerated gas were used to calibrate the PVT procedure for the effective gas temperature-to-volume ratio, thus accounting for the unknown gas temperature distribution in the torus and sub-divertor location of the gas diagnostics. The details of the respective

data analysis are given in Section 4. The introduction of the RGA-PVT procedure implied that ICWC had to be operated with cryogenic pumping, as opposed to the D→H changeover when only turbo-pumping with about factor 20 slower pumping rate was used. Furthermore, the number of ICWC pulses per day was limited by the total gas consumption of ~11 bar-l that could be allowed for the RGA-PVT procedure, governed by the limit on the measurable pressure rise upon regeneration of cryogenic pumps. The AGHS-imposed limit on the total daily amount of pumped hydrogenic gas of 90 bar-l also strongly limited the possible duration of GDC due to its high gas throughput. For that reason it was decided to perform GDCs in short (2 – 2.5 h) overnight slots after each day of ICWC, except the GDC on Sunday, when a 4 h long GDC phase was possible during the day time as there was no ICWC plasma operation on that day and no GDC in the nights before and after.

The experimental sequence of the T-removal campaign is shown in Figure 3. The upper colored line schematically shows the wall temperature evolution during the clean-up sequence. The first baking phase at lower temperature of 240 °C allowed a comparison of the efficiency of baking at different temperatures. The total baking time at 240 °C (days 1 to 3) was about 53 h and the duration of the 320 °C bake (days 4 to 9 with overlaid ICWC and overnight GDC) was about 120 h (excluding the temperature ramp up and ramp down phases). The low temperature phase at 110 °C was introduced during the last day of ICWC operation (day 10) to assess the efficiency of ICWC for fuel removal at a temperature close to that foreseen during ICWC operation in ITER (70 °C, i.e. the inlet temperature of the ITER cooling loop). Indeed, a clear reduction of D removal by ICWC in H with wall temperature decrease was seen during the D→H changeover experiment [13]. Subsequent diverted plasma operation on day 11 started already at the standard baseline wall temperature of 200 °C. The wall temperature ramp rates were about 5 °C/h for the warm-up and about -10 °C/h for the cool-down. The lower line in Figure 3 illustrates the cryogenic pumping conditions and schematically shows, on which days the RGA-PVT procedure was applied, which were essentially all ICWC days, including the one with cold wall (day 10), and the first day of diverted plasma operation (day 11).

The experimental sequence on days 5 to 8 and 10 can therefore be summarized as follows: (i) cooling down of cryo-panels in the early morning; (ii) execution of ICWC pulses up to the maximum T_2 gas consumption of ~11 bar-l; (iii) dwelling phase of about 2 h to allow for outgassing from the walls to be collected by the cryo-panels; (iv) regeneration of cryo-panels into the isolated torus; (v) RGA-PVT procedure for the regenerated gas with subsequent pumping down of the torus; (vi) GDC phase at night. After the GDC and pumping down of the torus the procedure continues with step (i) of the next day. It has to be noted that due to the need to find optimum matching conditions, the first full-

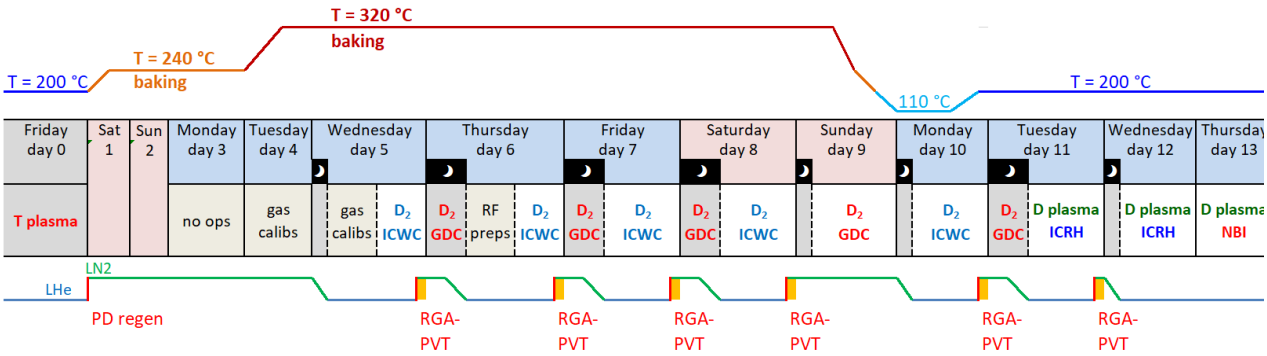

Figure 3. Experimental sequence of the T-removal campaign. The upper line schematically shows the evolution of the main vessel wall temperature with baking phases. The lower line shows the condition of divertor cryogenic pumping: PD stays for Pumped Divertor, LHe and LN2 indicate the phases with cryo-panels at liquid helium and liquid nitrogen temperatures, respectively. Also the schematic of tritium accounting on a daily basis using the RGA-PVT procedure is shown (see details in the text and analysis in Section 4.2). The moon shaped icons indicate that GDC cycles and subsequent cooling down of cryo-panels to LHe (also after RGA-PVT when no GDC followed) were executed overnight.

length reference power ICWC pulse could be executed only on day 7. Respectively, rather small amounts of gas were collected for the RGA-PVT on days 5 and 6, and tritium in the collected gas has to be attributed mostly to outgassing during baking.

The diverted plasma operation was performed on days 11, 12 and 13. First, low power ICRF heated plasmas with up to ~4.5 MW of radio-frequency (RF) power at 42 MHz (H minority heating scheme), toroidal magnetic field, Bt, of 2.5 – 2.6 T and plasma current, Ip, of 1.7 – 1.8 MA in different divertor configurations were applied to ensure the reduction of the plasma tritium content below 1%. Afterwards, plasmas with additional D-NBI heating were operated. For the first day of diverted plasma operation, the RGA-PVT procedure was applied, in order to compare the fuel removal with preceding ICWC days. For this reason the number of possible pulses was limited by the daily T_2 gas injection limit of ~11 bar-l. In total 5 pulses with RISP configuration (Figure 1a) were executed with the total flat-top plasma time of about 70 s (18 s for the last 3 pulses, while the first 2 pulses were shorter). After that, 6 limiter cycling pulses (Ip / Bt = 1.8 MA / 2.35 T) were executed, with low gas consumption and controlled plasma position alternately on the inner and the outer wall limiters. In the following two days, different divertor plasma configurations with ICRF and NBI heating were used: the so called vertical target (VT), corner-corner (CC) and Tile 5 (V5) configurations, characterized by different inner and outer strike points' positioning, as illustrated in Figure 1. In ICRF heated plasmas, short (200 ms) NBI blips at 1.5 MW were injected for the evaluation of the plasma tritium content from neutron yields. In the subsequent pulses, the NBI-heated phase was restricted to the first 10 s of the discharge, limited by the maximum allowed energy load on divertor tiles. The maximum achieved NBI heating power was 12.5 MW in the RISP configuration, 9.7 MW in VT, 11.0 MW in CC, and 9.6 MW in V5. We shall note that after the initial T removal experiment presented here, and a shutdown period of about 3 months, JET operations resumed with high power D plasma pulsing with total heating power up to 35 MW (NBI and ICRF).

Sub-divertor RGA quadrupole mass spectrometers [22] were used to quantify the isotopic content of the recovered neutral gas throughout the baking week, supported by a Penning discharge optical gas analyzer (OGA) [24, 25] during and after ICWC and divertor pulses. Figure 4 shows schematically the locations of the main chamber and sub-divertor gas diagnostics in JET. While high resolution Balmer α line spectroscopy in the plasma edge was used for the determination of the isotopic ratio in DT plasmas in TFTR [26] and in JET during DTE1 [27] and DTE2, its applicability to tritium content monitoring during the T-removal campaign was expectedly limited at low tritium content in plasma due to small separation and asymmetry of Doppler-broadened T_α and D_α spectral lines [28], and therefore will not be presented here. However, in NBI heated discharges, the plasma isotopic content could be inferred with high confidence from the ratio of the 14 MeV versus the total neutron production rates with the help of AFSI-ASCOT [29], which provides realistic fusion production rates and spectra for thermonuclear and fast-ion induced fusion reactions, and thus the calibration factor to calculate the isotopic ratio from the neutron production ratio. The total neutron production is measured in JET by $^{235}U/^{238}U$ fission chambers (KN1 diagnostics) [30], while the 14 MeV neutron production is measured with diamond and silicon diode detectors (KM7 diagnostics) [31, 32]. Furthermore, the time of flight spectrometer TOFOR (KM11 diagnostics) [33, 34] was used to measure the neutron spectrum encompassing both 2.5 MeV D-D neutrons and 14 MeV D-T neutrons along one vertical line of sight passing near the center of the core plasma. Finally, the temperature of plasma-facing surfaces in the divertor was monitored by the infrared (IR) thermography [35] and subsurface thermocouples [36] and characterized, in particular, the effectiveness of the RISP plasma configuration for heating of co-deposited layers in the divertor that stimulated thermal outgassing and isotope exchange.

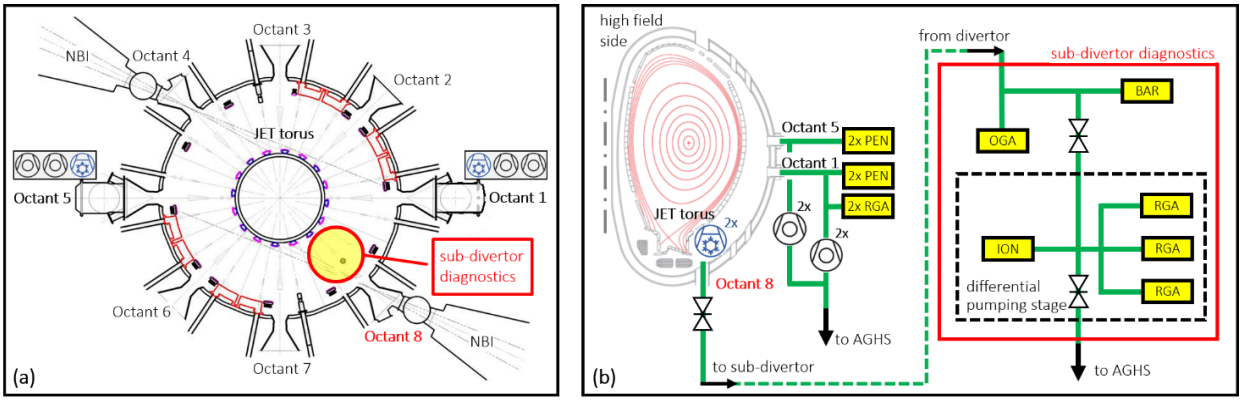

Figure 4. Schematic illustration of locations of turbo- and cryo-pumps and main chamber and sub-divertor neutral gas diagnostics in JET, namely RGA quadrupole mass spectrometers and the Penning discharge optical gas analyzer (OGA), together with an ionization pressure gauge (ION), a Baratron® capacitance manometer (BAR) and cold-cathode ionization gauges (PEN): (a) top view, (b) side view with a poloidal cross-section of the JET torus. Please note that this is not a complete Piping & Instrumentation Diagram so that only the main relevant pipelines, valves and instruments are schematically shown.

3. Isotopic content monitoring

The tritium content in the pumped gas measured by the sub-divertor OGA [24, 25] during and right after ICWC discharges and divertor plasma pulses is shown in Figure 5. On days 5 and 6, only few

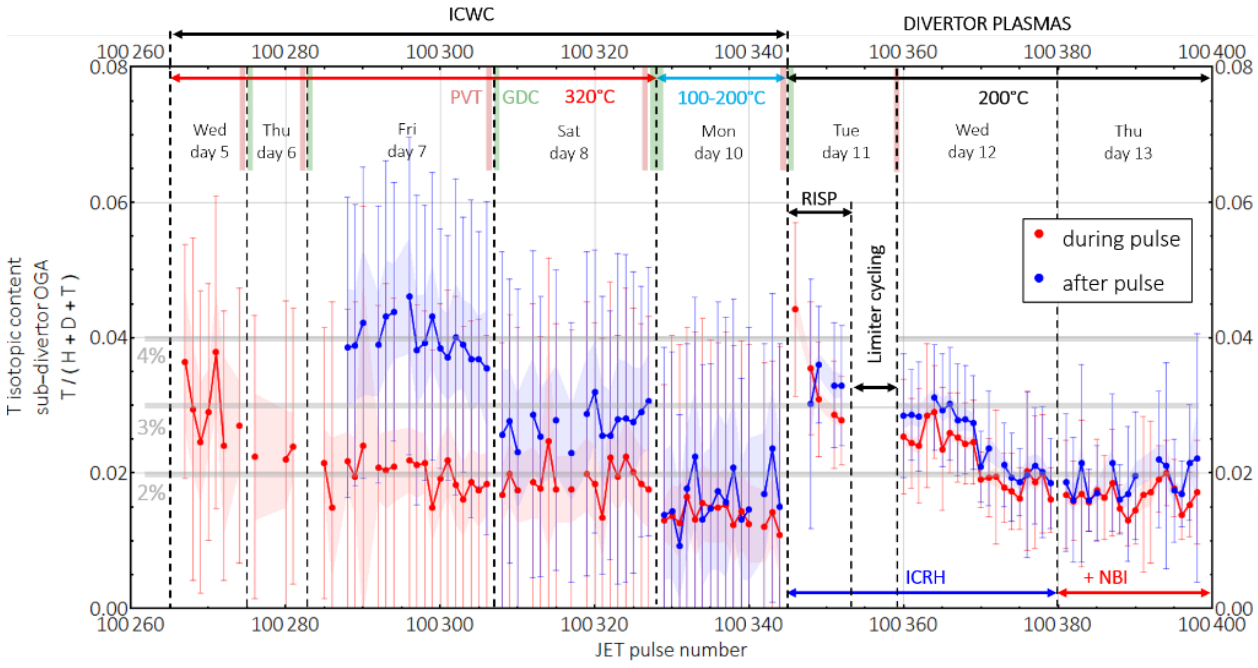

Figure 5. Tritium content T/(H+D+T) in the pumped gas measured by the sub-divertor OGA [24] during and after ICWC discharges and divertor plasma pulses. The color bars at the top axis with labels PVT and GDC indicate, respectively, RGA-PVT procedures performed in the evenings and overnight (but daytime on day 9) GDC phases. The error bars show the standard deviation of the mean (average of a set of data points during or after the pulse, respectively), while the color bands correspond to 99% confidence intervals for the mean. The scatter of data points in each pulse is much higher in case of ICWC pulses due to low gas pressure in the sub-divertor in these discharges resulting in a low signal intensity level (in number of CCD detector counts) and high signal to noise ratio.

short ICWC discharges were executed in order to improve matching of ICRF antennas for efficient coupling to the low density (typically 10^{17}-10^{18} m^{-3}) ICWC plasmas. Due to short interaction time between these ICWC discharges and wall surfaces, the neutral pressure in the post-discharge phase (i.e. once ICRF heating is switched off) was too low to enable measurements of the isotopic ratio T/(H+D+T) by OGA, so that only during-pulse OGA data is shown in Figure 5. From day 7 onwards, with longer ICWC discharges, a tritium fraction in the pumped gas of about 4% was measured in post-discharge, which is significantly lower than the initial deuterium fraction of ~15% measured in first ICWC pulses during the D→H changeover experiment [13]. This difference is explained by a two days longer baking phase and ~5 h of GDC that preceded the first full-length ICWC on day 7 as compared to first ICWC in [13]. There was only a small reduction of the isotopic content measured during and after the 17 full-length ICWC discharges operated on day 7. The isotopic content was reduced below 3% on day 8 (after about 2 h long overnight GDC) and remained almost constant throughout the day. Since the contribution of thermal outgassing by baking is expected to be negligible by that time, as will be shown in the next section dedicated to the T removal analysis, this reduction can be attributed to both ICWC discharges and overnight GDC phases, the effect of the latter on the T fraction being particularly visible in the post-discharge phase of ICWC plasmas in Figure 5. It has to be noted, however, that the detection limit of the sub-divertor OGA is determined by the resolution of the partially overlapping T_α and D_α spectral lines affected by the signal to noise ratio, especially at low light intensities, and is typically 1-2% T in D plasmas [24, 25]. On day 10, when the JET main chamber walls were cooled down to 110 °C in the morning and then gradually warmed up to 200 °C over the course of the day, the measured isotopic content fluctuated between 1% and 2% without any clear trend with respect to the number of operated ICWC pulses or wall temperature. The fact that the deduced isotopic fraction at cold wall remained constant and essentially the same during and after ICWC discharges indicates that the detection limit of the OGA system was probably reached. A similar situation was observed in diverted plasma pulses. Unlike ICWC discharges, the measured tritium content showed a clear reduction trend from ~3.5% to ~2% at first; however, soon leveled off around this value. This implies that essentially all values at ~2% are not to be trusted.

In diverted plasmas, starting with ICRF heating only, short (200 ms) NBI power injection blips made it possible to infer the T/(D+T) ratio from the neutron diagnostics. The results are shown in Figure 6a. A fast reduction of the isotopic content below the targeted value of 1% was observed during the first pulses, operated in the RISP configuration up to JET pulse number (JPN) #100352, and then alternately in all other configurations shown in Figure 1 (RISP, VT, CC, V5), until JPN#100383. Plasmas in limiter configuration (JPN#100353 to JPN#100358) were operated between these two series of diverted plasmas, although T/(D+T) could not be reliably inferred in that case, the 14 MeV neutron production rate being too low. The tritium fraction in plasma was further reduced by addition of NBI heating from JPN#100384 onwards, with a noticeable increase of T/(D+T) in RISP pulses JPN#100387 and JPN#100393 (the latter with 2.7 MW ICRF and 9 MW NBI during first 10 s), followed by a fast and drastic reduction of the isotopic content below the level of 0.1% in subsequent pulses (last pulse of the sequence JPN#100398). This indicates that the applied cleaning sequence and especially the high power RISP pulses were very efficient in reducing the tritium content in plasma. The tritium plasma content in plasma was further monitored by means of neutron rate measurements during the following deuterium campaign executed after three months of shutdown. Figure 6b shows the evolution of the tritium fraction in plasma over about 2 months of JET operation in this period, as well as in the next D campaign that followed after the helium campaign. In the restart phase after the shutdown, the tritium content ranged between ~0.1% and 1%, transiently increasing after longer breaks in plasma operation (e.g. over weekends) and after pulses with increased NBI heating power. After a couple of dozen of discharges with more than 10 MW NBI heating power, the isotopic content remained consistently below 0.3%, showing a general trend of further reduction well below 0.1%. Again a recovery to slightly higher values was observed after longer breaks in plasma operation, which has to be attributed to T diffusion from deeper surface layers during the breaks. Finally, after the He

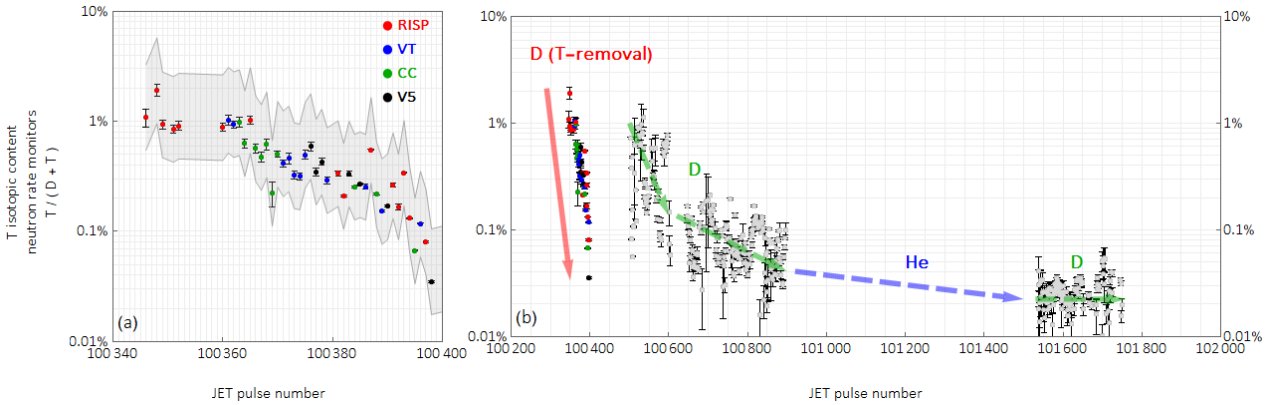

Figure 6. Tritium content inferred from neutron rates in divertor plasmas on days 12 and 13 of the experiment (a) and over the following months with two D campaigns separated by a He campaign (b). Data points along the red line in figure (b) correspond to the data from figure (a). The error bars show the statistical uncertainty dominated by 14 MeV neutron rates. The error bands on figure (a) illustrate the conservative estimate of the systematic uncertainty of a factor of 2, which is due to stability issues of 14 MeV neutron monitors and the response of fission chambers changing non-linearly with incident neutron spectra.

campaign, during which the tritium fraction could not be inferred reliably from neutrons, the tritium isotopic fraction stayed consistently below 0.06%. These data are in agreement with the data from the time-of-flight neutron spectrometer TOFOR [34], which estimates the tritium fraction to be of the order of 0.1% for pulses around JPN#100820.

4. Tritium fuel removal analysis

As the analysis of the gas collected by the AGHS system was not possible neither on a daily basis nor on the scale of the T removal experiment described here, the analysis of tritium fuel removal during baking, ICWC and GDC relies largely on the neutral gas diagnostics, namely on quadrupole mass spectrometers' data from sub-divertor RGAs. Several calibration procedures were performed in order to relate RGA signal intensities to partial pressures of gases of hydrogen isotopes and thus to allow quantitative assessment of RGA data. The calibration procedures were essentially different for the case of active torus pumping, such as during baking and ICWC, and for the case of the RGA-PVT procedure, when pumping was suspended and the torus was kept under relatively high pressure of about 0.1 mbar over an extended period of time (~1 h).

4.1 *Analysis of tritium removal by baking*

RGA calibration in the presence of active pumping would ideally require prolonged controlled gas injections into the torus so that both the torus pressure and the RGA mass signals stabilize for some time and allow to deduce the RGA sensitivity to each gas under steady state conditions. Such a setup was, however, not possible in JET during tritium operations, as the continuous gas injection valves are not tritium compatible and would require too high T_2 gas throughput. Therefore, RGA systems were calibrated by short gas injections using the integral method, in which RGA sensitivity, K_m, to a gas with molecular mass m is deduced from the integral of the RGA mass signal, J_m, in relation to the integral of the gas flow rate, i.e. from the total amount of the injected gas, Φ_m: $K_m = J_m/\Phi_m$. In such a way, for H_2, D_2 and T_2 admitted to the torus on by one, the sensitivities to masses 2, 4 and 6 (K_2, K_4 and K_6) were defined. The absolute values of K_m depend on the pumping conditions and may also depend on the pressure level in the torus, therefore cannot be directly applied for the calculation of partial pressures during baking, as the vacuum and pumping conditions can be different from those during the calibration. Moreover, in the case of a mix of hydrogen isotopes in the torus, masses 3 and 5 are also present, calibration factors for which are not directly known. However, for pure gas injections of H_2, D_2, and T_2 it was observed that under the same conditions relative RGA sensitivities

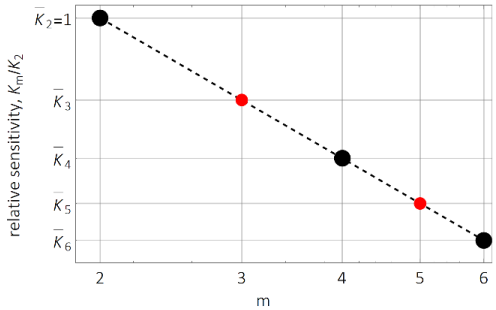

Figure 7. Illustration of the power law dependence of relative RGA sensitivities to different masses (normalized by the sensitivity to mass 2). The slope of the line in the double logarithmic scale is obtained from measured sensitivities to masses 2, 4 and 6 in single gas injections of H_2, D_2 and T_2, respectively. Relative sensitivities to massed 3 and 5 are assumed to fall on the same line.

$\bar{K}_m = K_m/K_2$ (normalized by the sensitivity to mass 2) for masses 2, 4 and 6 show a $\bar{K}_m = (2/m)^\beta$ power law dependence with a positive value of the exponent, $\beta > 0$, which is usually attributed to a combined effect of the ionization probability, ion extraction, quadrupole transmission and electron multiplier gain factors [37, 38]. In other words, relative sensitivities fall on a line with a negative slope on a $\log(\bar{K}_m)$-vs-$\log(m)$ plot (Figure 7), and therefore also the relative sensitivities to masses 3 and 5 can be estimated from the power law dependence as shown in Figure 7. Knowing relative sensitivities to masses 2 ($\bar{K}_2 = 1$ by definition) to 6, the absolute values of partial pressures of isotopic molecules with respective masses during baking, p_m, are calculated by applying relative calibration factors to each RGA mass signal, I_m (background subtracted), to obtain relative pressures, $\bar{p}_m$, and scaling the result to recover the total measured gas pressure in the torus, p_{torus}:

$$\bar{p}_m = I_m/\bar{K}_m,$$

$$p_m = \frac{\bar{p}_m}{\sum_m \bar{p}_m} p_{\mathrm{torus}}.$$

In this approach RGA sensitivities to D_2 and HT, both contributing to RGA signal at mass 4, are assumed to be equal. In order to disentangle the contributions of D_2 and HT to p_4, instantaneous equilibrium between H_2, T_2 and HT is calculated based on temperature dependent equilibrium constants [39]. The amount of tritium atoms removed from the vessel during baking was then estimated as the sum of properly scaled integrals of partial pressures of tritium containing species (DT + $2T_2$ + HT) multiplied by the average pumping speed (deduced from pressure decay after gas injections and taken to be 5 m^3/s during baking when only turbo-pumps were active). An example of time traces of measured mass signals from one of RGA systems is shown in Figure 8, alongside with the torus pressure and wall temperature evolution. Calculations were performed using data from three sub-divertor RGA systems, four torus pressure gauges and different gas injection tests described above. From these datasets, mean values of the removed tritium and standard deviations (as a measure of uncertainty) were calculated for different phases of baking on days 1-5, including extrapolated 240 ºC baking trends for days 3-9 and extrapolated 320 ºC baking trends for days 5-9). The results are summarized in Figure 9 and Figure 11, together with respective results for T removal in RGA-PVT and by GDC. It has to be noted that the analysis of tritium removal in GDC is nontrivial, because of the high deuterium gas throughput and correspondingly high deuterium contribution to mass signals, in which, for example, formation of D_3^+ in the RGA system itself (thus dominating at mass 6 otherwise associated with T_2^+) cannot be excluded. Therefore, in the analysis conservatively only mass 5 signal was taken into account and assumed to correspond entirely to DT.

4.2 RGA-PVT analysis of tritium removal by ICWC and RISP

Calibration of sub-divertor RGA systems in the presence of different mixtures of all three hydrogen isotopes (H, D, T) under conditions relevant for the RGA-PVT procedure, namely with an isolated

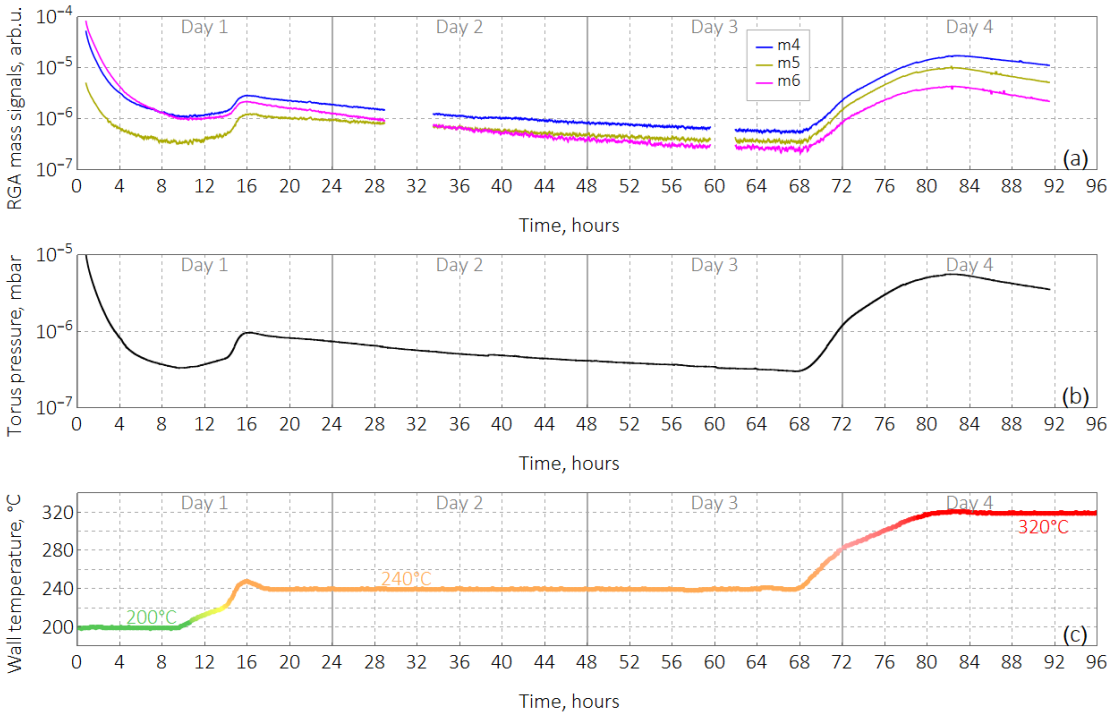

Figure 8. Examples of time traces of measured mass signals (m2 and m3 omitted for better readability) from one of RGA systems (a), torus pressure (b), and wall temperature (c) during first days of baking.

torus pumping, was performed prior to T and DT plasma campaigns. Controlled gas injections of different hydrogen isotopes into the isolated torus were used that resulted in a gradual stepwise increase of the torus pressure. Four series of gas injections were performed varying the injection order and quantity of H_2, D_2 and T_2. The applied calibration model assumes instantaneous equilibria among the isotopic hydrogen molecules H_2, HD, D_2, DT, T_2 and HT calculated based on temperature dependent equilibrium constants [39] using the known amounts of injected gases in form of H_2, D_2 and T_2.

During RGA-PVT procedures, sub-divertor RGA systems were used to estimate the fraction of tritium containing molecules in the gas regenerated from the divertor cryo-panels, while the total amount of released gas was derived from the related total torus pressure rise. The PVT gas balance (collected vs injected) and this way estimated total amounts of removed tritium in each of five RGA-PVT sessions of the corresponding days of the experiment are summarized in Figure 9. In all sessions except the one with ICWC at reduced wall temperature (day 10), more gas was collected than it was supplied to the torus (Figure 9a). The excess gas has to be attributed to outgassing and the effect of the isotope exchange. The fact that less gas is collected after ICWC on day 10 indicates strong wall pumping at reduced wall temperature after depletion of the wall reservoir by preceding baking and cleaning by ICWC and GDC. Since the gas collected by cryogenic pumps and analyzed by RGA-PVT includes also the contribution of outgassing from the walls by baking in the absence of plasma operation and in between plasma pulses, this contribution had to be separated from the effect of ICWC

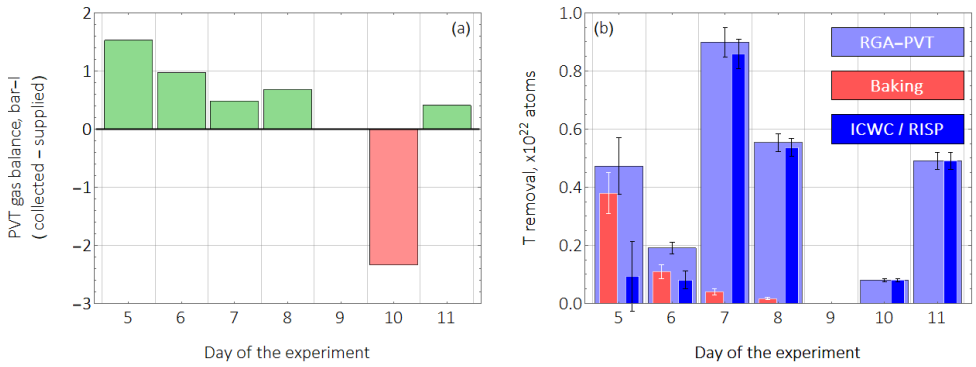

Figure 9. (a) The PVT gas balance (the difference between the collected and injected gas) for each of respective sessions of plasma operation analyzed by RGA-PVT on the days of the experiment; and (b) the corresponding amounts of recovered tritium quantified via the RGA-PVT procedure compared to the estimated amount of tritium attributed to outgassing from the walls by baking over the gas collection time corresponding to ICWC sessions (days 5-8 and 10, ~12.5 h per day) and first RISP plasma sessions (day 11).

and diverted plasmas and is also shown in Figure 9b. Thus, tritium removal attributed to ICWC is given by the difference between the total amount of tritium recovered in RGA-PVT and the respective estimate of outgassing as shown in Figure 9b, following the extrapolated outgassing trends of the initial baking phase (from day 4 in Figure 8).

4.3 Comparison of tritium removal by different methods

Cumulative tritium removal by different methods (baking, ICWC, GDC) is shown in Figure 10. The curves clearly indicate that baking at 320 ºC allowed removing about twice more tritium compared to baking at 240 ºC, extrapolated to the same duration. While removal by baking levels off at around day 6, ICWC and GDC have a clear added effect. It has to be understood that, although shown together in Figure 10, ICWC sessions followed by RGA-PVTs were executed before GDCs. This is illustrated by the order of respective bars in Figure 11. As it was mentioned in Section 2, first full-length reference power ICWC pulses were executed only on day 7. Therefore, T removal deduced from RGA-PVT on days 5 and 6 is attributed largely to the effect of baking, as can be seen from Figure 9b and Figure 10. In Figure 11, outgassing during baking is shown in 24 h slots, therefore corresponding bars on days 5 and 6 are higher than the RGA-PVT bars. On the contrary, in Figure 9b and Figure 10, outgassing during baking is restricted to the duration of gas collection in respective ICWC sessions (~12.5 h). Noteworthy, tritium removal by GDC on days 5 and 6 exceeds that by baking. The contribution of baking decreases quite rapidly with time, so that T removal on subsequent days 7 and 8 is mostly due to ICWC plasma pulsing and exceeds that of GDC. Until the end of the baking phase on day 9, ICWC and GDC allowed to remove about 65% more tritium than baking alone. This result is in general agreement with observations from the D→H changeover experiment [13]. On day 10, when vessel walls were cooled down to 110 ºC and then gradually warmed up to 200 ºC, ICWC showed a significantly lower T removal. This can be attributed to depletion of the accessible wall reservoir due to preceding cleaning, including GDC on day 9, but also to less effective isotope exchange at lower wall temperatures [40]. Subsequent GDC after day 10, surprisingly, showed comparable T removal as on days 8 and 9. This may indicate delayed T diffusion from deeper bulk that was slowed down at low wall temperatures on day 10. Significantly higher tritium removal observed in RGA-PVT on day 11 is due to first diverted plasma pulses in RISP configuration that accessed different wall surfaces, in particular co-deposited layers in the upper part of the inner divertor. However, the quantitative analysis of tritium removal by diverted plasmas was not performed on days 12 and 13, for the reasons explained in Section 2 (limitations on gas collection).

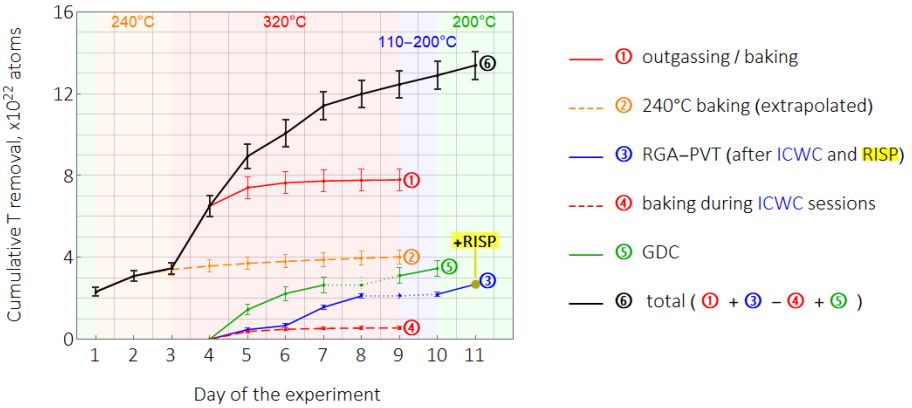

Figure 10. Cumulative tritium removal by different methods over the days of the experiment. Removal by outgassing was deduced from the sub-divertor RGA data up to day 4 and extrapolated from the respective RGA data trends for the remaining period of baking. Dotted lines for removal in RGA-PVT and by GDC indicate that there was no RGA-PVT on day 9 and no GDC on day 8. Tritium removal by ICWC alone is not directly shown and has to be understood as the difference between curves 3 and 4 (see Figure 9b). Although chronologically GDC sessions were performed overnight and are shown in Figure 3 on days 6, 7, and 8, the respective data points in this figure are shown for better representation on days 5, 6, and 7.

Cumulative fuel removal by ICWC and GDC is represented in Figure 12 as a function of the total energy throughput, E. The points correspond to the accumulated tritium removal day by day (from Figure 10). The last two points on the combined plot correspond to the gains of the removed amount on day 10, i.e. in ICWC at cold wall and GDC at 200 ºC. The removal is reasonably described by an envelope curve $\sim E^{0.5}$ observed in past ICWC experiments at JET [41]. Both, ICWC and GDC gains fit the curve. However, GDC seems to provide additional removal compared to ICWC. This can be attributed to additional removal due to different plasma-wall interaction areas and higher efficiency of GDC, or to an overestimation of T removal by GDC. The total amount of removed tritium is about a factor 4 lower than the total amount of deuterium removed during the D→H changeover experiment [13] at the same total energy injected. This can be explained, however, by the fact, that tritium accounts only for half of the fuel in DTE2 and that significantly less tritium was injected into the torus during tritium and deuterium-tritium campaigns as compared to deuterium injected in previous JET experimental campaigns. Figure 13 shows the total amounts of injected hydrogen isotopes though the T and DT campaigns (C39-41, right figure axis) and in the directly preceding D campaigns (C38, left figure axis). Note that the scale of the left axis (for D campaigns) is 10 times the scale of the right axis (for T and D-T campaigns). The walls in JET are strongly loaded with deuterium even if there are intermediate routine cleaning and dedicated isotope-exchange treatments undertaken.

The total quantifiable cumulative T removal by all methods over the course of days 1 to 11 of the

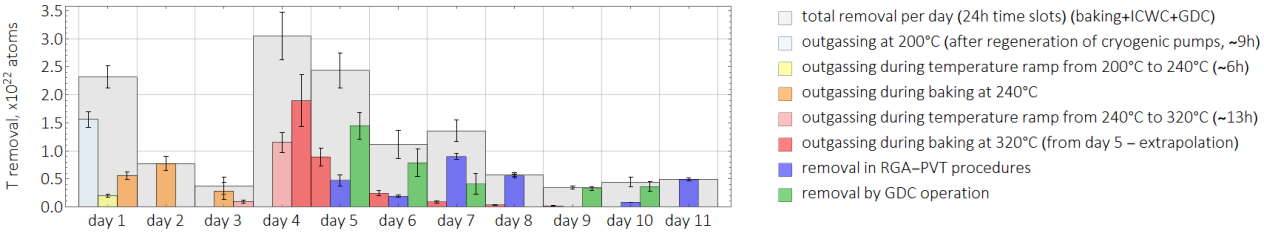

Figure 11. Estimated tritium removal during different cleaning and baking phases, including extrapolation of outgassing trends at different baking temperatures, calculated per day (24 h time slots). Note: Although chronologically GDC sessions were performed overnight and are shown in Figure 3 on days 6, 7 and 8, the respective data points in this figure are shown for better representation on days 5, 6 and 7. The actual chronological order of RGA-PVT and GDC can be recovered from the order of respective bars in the graph.

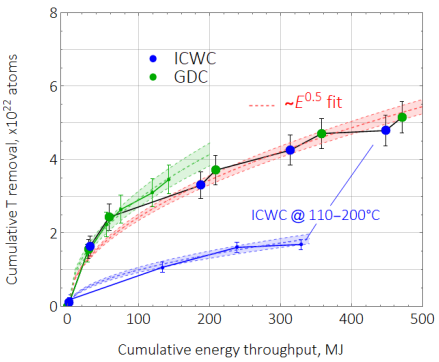

Figure 12. Cumulative tritium removal by ICWC and GDC as a function of the total discharge energy throughput, E. Dependencies for GDC and ICWC alone are shown, as well as the combined data. The dashed envelope curves are fitted as $\sim E^{0.5}$ as was observed in past ICWC experiments at JET [41].

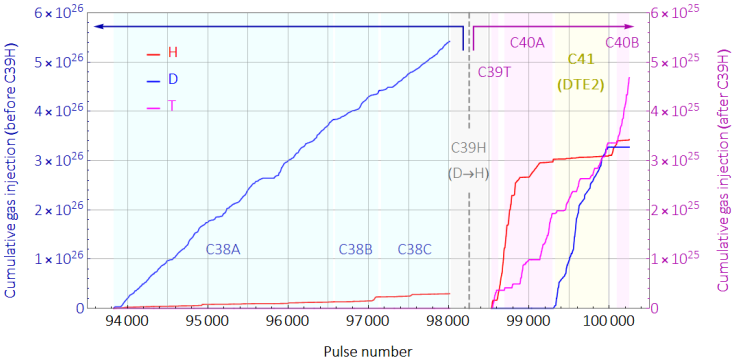

Figure 13. Cumulative amounts of injected hydrogen isotopes in different experimental campaigns. The left part of the graph (before C39H) shows the last deuterium campaigns. The right part of the graph (after C39H) shows the recent tritium and deuterium-tritium campaigns. The C39H campaign started with the D→H changeover experiment [13]. Note the different scales of the vertical axes for the data before and after C39H as indicated by arrows.

experiment was $(13.4 \pm 0.7) \cdot 10^{22}$ atoms or (0.67 ± 0.03) g, with ~58% attributed to baking, ~12.5% to ICWC, ~26% to GDC, and ~3.5% to first low power RISP plasmas on day 11. The uncertainty is given by the standard deviation as described in Section 4.1. This amount of tritium can be compared to results of global tritium accounting by the JET tritium reprocessing plant, in which the total amount of on-site T prior to start of T operations is compared to the verified T amount within the AGHS main process subsystems, including the collected tokamak exhaust and accounting for the radioactive T decay. The difference is tagged as the unaccounted tritium inventory and, apart from the actual in-vessel hold up, includes also numerous discreet inventories within the AGHS that cannot be directly quantified, such as water ice in the impurity processing system and many secondary getter beds to trap permeated tritium, and require months for T recovery. According to AGHS accounting, the amount of unaccounted tritium assessed 3 weeks before the T-removal experiment went down by 0.71 g when assessed after the T-removal experiment (T decay already taken into account and thus excluded from the result), which is in very good agreement with T removal estimates presented here.

4.4 Mechanisms of T removal at play in RISP plasmas

Diverted plasmas with raised inner strike point (RISP configuration, Figure 1a) are currently considered to be used in ITER to remove tritium from co-deposited layers in the inner divertor [42] that are expected to build up there, similarly to JET-ILW. Fuel removal in this case can be driven by two cooperating processes. On one hand, shifting the inner strike point towards the thickest co-deposited layers will lead to erosion of those layers by high flux D plasma, promoting at the same time T→D isotope exchange. On the other hand, high flux plasma exposure will lead to a significant rise of the surface temperature due to poor thermal contact between the co-deposited layer and substrate [43], as observed in JET-ILW, thus stimulating thermal outgassing.

In the case of layer erosion, which in the case of RISP plasmas in JET-ILW is estimated to be at least of the order of 10 nm/s, an important question is the re-deposition of the eroded material and related fuel re-co-deposition, i.e. whether fuel is removed or re-deposited at more remote locations. This question is being addressed by the ERO2.0 code [44] simulations, for which plasma background in the inner divertor region is provided by the OEDGE code [45] using boundary conditions from divertor Langmuir probe data. Results of these investigations are to be published elsewhere.

In this section, we will focus on the case of thermal outgassing stimulated by layer heating by plasma. Figure 14 shows the surface temperature evolution on the top of the inner divertor (Tile 1,

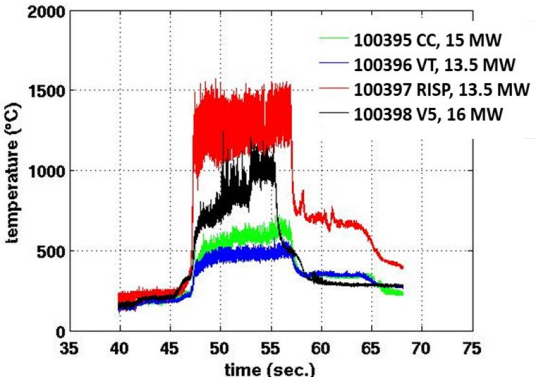

Figure 14. Tile 1 surface temperature evolution measured with IR thermography in NBI-heated diverted plasmas on day 13. Line colors and information in the legend correspond to plasma configurations shown in Figure 1.

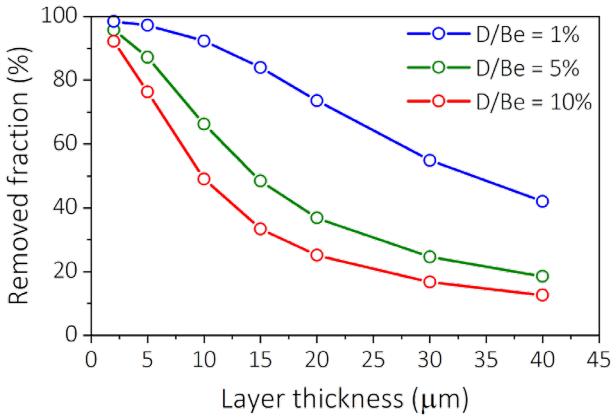

Figure 15. CRDS simulation results of fuel removal from co-deposited Be layers of different thickness and D content when exposed to a single high-temperature excursion corresponding to the surface temperature evolution in a high-power RISP plasma pulse (Figure 14).

Figure 1a) as measured with the IR thermography in NBI-heated diverted plasma pulses on day 13 (IR vs thermocouples analysis similar to the one in [43]). The line colors and information in the legend in the figure correspond to different plasma configurations as shown in Figure 1. Using the experimental surface temperature evolution in high-power NBI-heated RISP plasma (red curve in Figure 14: T_{max} ~1280 °C, duration ~10 s), CRDS code [46] simulations have been executed. CRDS is a reaction-diffusion code describing the time evolution of concentration profiles of solute and trapped hydrogen isotopes in a material by solving a system of coupled rate equations, accounting for ion implantation and material temperature evolution. The profile of trapping sites was assumed uniform through the entire thickness of the co-deposited layer. No flux boundary condition was used at the boundary with substrate (i.e. no diffusion into substrate). Three trap types with the following de-trapping energies and relative contributions were used that reproduced reasonably well a thermal desorption spectrum (TDS) from one of JET-ILW Tile 1 samples analyzed in the lab: 1) 0.75 eV (25%); 2) 1.12 eV (30%); 3) 1.3 eV (45%). All other D diffusion and trapping parameters were taken from [16]. Simulations of outgassing during the imposed temperature excursion in a single discharge were performed for different layer thicknesses and initial D contents. The resulting fraction of removed fuel as a function of the layer thickness is shown in Figure 15 for three different values of the initial D content: 1%, 5% and 10%. While for thin layers fuel removal is very efficient (>90%), fuel removal efficiency decreases strongly with layer thickness and with increase of the initial D content in the layer. For a 40 μm thick layer (i.e. the largest thickness of Be layers measured post-mortem on the top inner divertor [14]), less than 50% of fuel is removed in the case of initial D/Be = 1% and only about 15% is removed for initial D/Be = 10%. All in all, for moderately thick layers of <10 μm with initial D content <5% as observed for JET-ILW samples from Tile 1, solely the heating of divertor surfaces by plasma during RISP pulses can lead to significant fuel removal from co-deposited layers by thermal outgassing (>65%). Additional fuel removal associated with erosion can be expected to further reduce the residual T content in the layers.

5. Summary and implications for ITER

A tritium removal sequence was qualified prior to T operations in JET-ILW and was conducted after the DTE2 and T campaigns. It started with 4 days of baking, first at 240 °C and then at 320 °C. ICWC plasma pulsing in D was applied during subsequent days of extended baking at 320 °C. Short D_2-GDC cleaning cycles of 2 to 4 h duration were executed overnight. After the week of baking combined with ICWC and GDC, diverted plasma operation at a main chamber wall temperature of

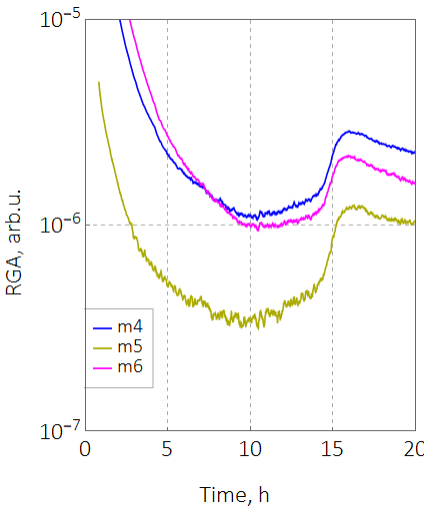

Figure 16. Zoom-in of time traces for the first 20 hours of data shown in Figure 6a.

200 °C was resumed in deuterium using different strike point configurations, including RISP, and different heating schemes (ICRF and NBI) and power (up to ~16 MW). The efficiency of cleaning methods was assessed by measuring the amount of tritium removed and by the evolution of the isotopic ratio in plasmas and in the residual gas. The isotopic content in ICWC plasmas was already low (~4%) after the first days of baking and was further reduced below 3% over the course of two days of ICWC operation (with GDC in between) at the wall temperature of 320 °C as evaluated by the sub-divertor optical gas analysis system (Figure 5). The isotopic fraction T/(H+D+T) in ICWC plasmas at wall temperatures 110 – 200 °C stayed almost constant at the level of 1.5%, indicating probable resolution limit of the detection system. The T fraction in diverted plasmas measured by the sub-divertor optical gauge showed a similar behavior. Gradual increase of the plasma heating power by means of NBI heating facilitated monitoring the isotopic content inferred from D-T and D-D neutron rates. A drastic decrease of the isotopic content from ~1% to well below 0.1% was observed after high power (up to 12.5 MW) plasma operation in RISP configuration (Figure 6a). The T clean-up campaign continued after a planned 3-months long shutdown, with D plasma operation with up to 35 MW heating power, in which consistently low levels of tritium in plasma were measured (Figure 6b).

Tritium removal during the initial cleaning phase described in this contribution was estimated to be $(13.4 \pm 0.7) \cdot 10^{22}$ atoms or (0.67 ± 0.03) g, based on the RGA data and using the specially developed RGA-PVT technique for gas collection and analysis. The removal by different methods is compared in Table 1 with results of the D→H changeover experiment [13], which laid the basis for the actual tritium cleaning sequence. The total amount of removed tritium is significantly lower than the amount of removed deuterium reported in [13], however this is an expected result due to the fact that both isotopes were injected into plasma throughout DTE2 and that significantly larger amounts of deuterium were used in the preceding JET campaigns (Figure 13). The cleaning efficiencies of ICWC, GDC and RISP plasmas in terms of their contribution to fuel removal are very comparable in the case of D and T removal. However, the contribution of baking is smaller for the case of tritium. Since the data for ICWC shown in Table 1 includes the contribution of baking, it can be concluded that the contribution of ICWC alone (i.e. assessed with baking excluded) was lower in the case of deuterium. The reason for this reduction is a faster decay of tritium outgassing during baking compared to deuterium outgassing, as can be seen from RGA mass signal trends in Figure 16, representing a zoom-in of Figure 8a for the first 20 hours of outgassing, including the wall heating up to 240ºC. Shortly after plasma operation and regeneration of cryogenic pumps, outgassing is dominated by tritium (mass 6). However, already during the initial phase of baking the situation changes and outgassing becomes dominated by deuterium (mass 4). Most probably, the reason for that is the already mentioned significant wall loading by deuterium in preceding experimental campaigns. While tritium is retained relatively close to the surface, deuterium starts to diffuse also from deeper bulk of the wall material

Changeover	Total	Baking ("measured" part)	Baking (extrapolated part)	ICWC (including baking)	GDC	First RISP plasmas (low power pulses)
D → H	5.3×10^{23}	2.9×10^{23} (57%)	1.2×10^{23} (24%)	0.9×10^{23} (18%)	1.3×10^{23} (25%)	2.4×10^{22} (5%)
T → D	1.3×10^{23}	6.1×10^{22} (46%)	1.7×10^{22} (12%)	2.2×10^{22} (17%)	3.5×10^{22} (26%)	0.5×10^{22} (3%)

Table 1. Comparison of tritium removal by different methods after DTE2 to deuterium removal in D→H changeover experiment [13]. The reader is referred to Section 4.1 for the explanation of the "measured" and "extrapolated" parts of removal by baking. First RISP plasmas imply the first 5 low power pulses after ICWC as described in Section 2.

and in the long run starts to be the dominant contributor to outgassing. At the same time, one should not exclude a possible isotope effect on retention, in which heavier T atoms can be preferentially trapped at material defects. This will also reduce the rate of tritium release. The fact that the isotopic content in plasma could be reduced quite fast is promising; however, it indicates only low tritium release into plasma and not low residual tritium amount in the walls. As the final result of tritium accounting by AGHS is not yet available, no conclusion can be drawn at the moment regarding the overall in-vessel tritium inventory after the DTE2 and T campaigns. Indeed, processing and quantification of tritium from the AGHS uranium getter beds that capture permeated hydrogen isotopes and of tritiated water ice in the cryogenic fore-vacuum and impurity processing systems [21] are still on-going. Even when completed, the result of T accounting, the primary aim of which is to quantify the amount of tritium retained within the JET plant, must be distinguished from the in-vessel T retention in JET-ILW accessible by T-removal methods in this experiment. Unfortunately, the in-vessel T retention in JET-ILW is still not assessed experimentally. Gas balance experiments with RGA-PVT in T similar to those done in D in [4, 12] were inconclusive due to technical issues, and new attempts are under discussion. As for the long-term T retention, its evaluation from the post-mortem analysis of JET PFCs will be possible only after JET has ceased operations. Retention values from past deuterium campaigns can, however, be used to give lower and upper bounds on the in-vessel T retention. The gas balance analysis of the D fuel retention in earlier D campaigns in JET-ILW has shown the retention fraction to be about 2% of the injected amount for a range of plasma scenarios [4, 12]. This upper-limit value is based on one day of plasma operations and thus does not take the long-term outgassing into account, such as overnight and during longer breaks in operation. For the total 252 g of tritium injected during the DTE2 and T campaigns, this results in 5.04 g of in-vessel retained T and the tritium cleaning efficiency of $0.67/5.04 = 13.3\%$. Taking into account longer breaks in operation between campaigns (full T → D-T → full T) and occasional routine GDC cycles, a significantly lower retention fraction can be expected. As a lower bound, the long-term D retention in JET-ILW of 0.19% [14] can be taken for reference. This will result in 0.48 g of retained T, which is below the value of 0.67 g removed by the cleaning measures presented here.

What can be noted regarding different cleaning methods applied for T removal is, first of all, that baking at 320 °C is more effective than baking at 240 °C, allowing removing about a factor two more tritium (Figure 10). Then, while removal by baking almost levels off after 4-5 days, ICWC and GDC promote additional removal, which follows roughly a $\sim E^{0.5}$ envelope of cumulative removal as a function of the total cumulative energy throughput, E (Figure 12). Finally, RISP plasma operation proved to be very efficient in removing fuel from co-deposited layers in the inner top divertor. A positive correlation was observed between the Tile 1 surface temperature and the plasma tritium content (inferred from neutron yield monitors) in first RISP plasmas. A drastic reduction of the isotopic content in subsequent pulses suggests that almost complete tritium release from co-deposited layers on Tile 1 could be achieved. Preliminary assessment of thermally assisted fuel release in RISP pulses by means of reaction-diffusion modelling with the CRDS code indicates that strong (>65%) degassing of co-deposited layers is possible in one single RISP plasma discharge for moderate layer thicknesses (≤10 μm) and D contents (≤5%). In addition to outgassing, erosion of T rich Be layers in the divertor certainly contributes significantly to fuel removal by RISP plasmas. Simple estimation of physical sputtering for given plasma fluxes deduced from Langmuir probe measurements leads to erosion rates of at least 10 nm/s. However, re-deposition of eroded material has to be taken into account since it may lead to repeated fuel co-deposition at more remote locations. This topic is being addressed by dedicated ERO2.0 simulations and will be published elsewhere.

Fuel removal during plasma operation periods will be mandatory in ITER [47], in addition to baking and GDC that will be applied between campaigns (in the absence of the toroidal magnetic field and cooling of the superconducting coils), as baking and GDC will be less effective if thick tritiated deposited layers will be formed. For fuel recovery from the main chamber in ITER, ICWC is

considered, applied with the toroidal field and providing uniform neutral atom fluxes to the main chamber walls, in addition to the ion fluxes at field lines intersecting with wall components. For ICWC applied as sequences of short pulses with low duty cycle, the time averaged uniform wall flux is similar to the wall ion flux in GDC [47], thus facilitating isotope exchange also in recessed areas. While ICWC will be ineffective for the divertor cleaning, JET-ILW results on T removal by RISP plasma operation give positive prospects on the feasibility of T removal from co-deposited layers in the actively cooled divertor of ITER even due to the heating effect alone, provided that these layers will have comparably poor thermal contact with W substrate as in JET-ILW. As for JET-ILW, simulations of layer erosion and tritium re-deposition in RISP plasma configuration are required to form a more complete picture of tritium migration in the divertor during this tokamak scenario. In RISP pulses in JET-ILW, the pumping efficiency of the released isotopes is low. Similarly, in ITER the released T will likely be co-deposited or implanted in plasma-facing surfaces. It is therefore proposed to interlace divertor cleaning pulses with ICWC, to deplete the near surface inventory and recover the released T.

Acknowledgements

This work has been carried out within the framework of the EUROfusion Consortium, funded by the European Union via the Euratom Research and Training Programme (Grant Agreement No 101052200 — EUROfusion). Views and opinions expressed are however those of the author(s) only and do not necessarily reflect those of the European Union or the European Commission. Neither the European Union nor the European Commission can be held responsible for them.

References

[1] G.F. Matthews et al, Phys. Scr. T145 (2011) 014001, DOI: 10.1088/0031-8949/2014/T159/014009

[2] C.F. Maggi et al, Nuclear Fusion Special Issue of IAEA Fusion Energy Conference 2023 (2024)

[3] M. Keilhacker, Phil. Trans. R. Soc. Lond. A 357 (1999) 415, DOI: 10.1098/rsta.1999.0335

[4] T. Loarer et al, J. Nucl. Mater 438 (2013) S108, DOI : 10.1016/j.jnucmat.2013.01.017

[5] P. Andrew et al, Fus. Eng. Design 47 (1999) 233, DOI: 10.1016/S0920-3796(99)00084-8

[6] L. Horton et al, Fus. Eng. Des. 109–111 (2016) 925–936, DOI: 10.1016/j.fusengdes.2016.01.051

[7] J. P. Coad, J. Nucl. Mater. 226 (1995) 156, DOI: 10.1016/0022-3115(95)80021-2

[8] D. Mueller et al, J. Nucl. Mater. 241-243 (1997) 897, DOI: 10.1016/S0022-3115(97)80162-6

[9] C. H. Skinner et al, J. Vac. Sci. Technol. A 14 (1996) 3267, DOI: 10.1116/1.580224

[10] G. Federici et al, J. Nucl. Mater. 266–269 (1999) 14, DOI: 10.1016/S0022-3115(98)00876-9

[11] J. Roth et al, Plasma Phys. Control. Fusion 50 (2008) 103001, DOI: 10.1088/0741-3335/50/10/103001

[12] S. Brezinsek et al, Nucl. Fusion 53 (2013) 083023, DOI: 10.1088/0029-5515/53/8/083023

[13] T. Wauters et al, Phys. Scr. 97 (2022) 044001, DOI: 10.1088/1402-4896/ac5856

[14] A. Widdowson et al, Phys. Scr. 97 (2022) 124075, DOI: 10.1088/1402-4896/ac3b30

[15] K. Heinola et al, Nucl. Fusion 57 (2017) 086024, DOI: 10.1088/1741-4326/aa747e

[16] G. De Temmerman et al, Nucl. Mater. Energy 12 (2017) 267, DOI: 10.1016/j.nme.2016.10.016

[17] A. Založnik et al, Nucl. Mater. Energy 24 (2020) 100750, DOI: 10.1016/j.nme.2020.100750

[18] D. Douai et al., J. Nucl. Mater. 415 (2011) S1021, DOI: 10.1016/j.jnucmat.2010.11.083

[19] D. Douai et al., J. Nucl. Mater. 438 (2013) S1172, DOI: 10.1016/j.jnucmat.2013.01.259

[20] D. Kogut et al, Plasma Phys. Control. Fusion 57 (2015) 025009, DOI: 10.1088/0741-3335/57/2/025009

[21] R. Lässer et al, Fusion Eng. Des. 47 (1999) 173, DOI: 10.1016/S0920-3796(99)00082-4

[22] U. Kruezi et al, JINST 15 (2020) C01032, DOI: 10.1088/1748-0221/15/01/C01032

[23] E. Bertolini, Fusion Eng. Des. 30 (1995) 53, DOI: 10.1016/0920-3796(94)00401-R

[24] S. Vartanian et al, Fus. Eng. Design 170 (2021) 112511, DOI: 10.1016/j.fusengdes.2021.112511

[25] C.C. Klepper et al, Nucl. Fusion 60 (2020) 016021, DOI: 10.1088/1741-4326/ab4c5a

[26] C. H. Skinner et al, J. Nucl. Mater. 241–243 (1997) 887, DOI: 10.1016/S0022-3115(97)80160-2

[27] A. C. Maas et al, Fusion Eng. Des. 47 (1999) 247, DOI: 10.1016/S0920-3796(99)00085-X

[28] V. Neverov et al, Nucl. Fusion 59 (2019) 046011, DOI: 10.1088/1741-4326/ab0000

[29] P. Sirén et al, Nucl. Fusion 58 (2018) 016023, DOI: 10.1088/1741-4326/aa92e9

[30] D.B. Syme et al, Nucl. Eng. Design 246 (2012) 185–90, DOI: 10.1016/j.nucengdes.2011.08.003

[31] M. Angelone et al, Rev. Sci. Instrum. 76 (2005) 013506, DOI: 10.1063/1.1834691

[32] C. Cazzaniga et al, Rev. Sci. Instrum. 85 (2014) 043506, DOI: 10.1063/1.4870584

[33] M. Gatu Johnson et al, Nucl. Instrum. Methods A 591 (2008) 417–30, DOI: 10.1016/j.nima.2008.03.010

[34] B. Eriksson et al, Plasma Phys. Control. Fusion 64 (2022) 055008, DOI: 10.1088/1361-6587/ac5a0d

[35] I. Balboa et al, Rev. Sci. Instrum. 87 (2016) 11D419, DOI: 10.1063/1.4960323

[36] C. Guillemaut et al, Nucl. Mater. Energy 12 (2017) 234, DOI: 10.1016/j.nme.2017.02.010

[37] N.R. Reagan et al, J. Vac. Sci. Technol. A 5 (1987) 2389, DOI: 10.1116/1.574460

[38] J.W. Pyper et al, Technical Report UCRL-52391, Lawrence Livermore National Laboratory, United States, 1978, DOI: 10.2172/5043666

[39] W. M. Jones, J. Chem. Phys. 17 (1949) 1062, DOI: 10.1063/1.1747113

[40] D. Kogut et al, Phys. Scr. T167 (2016) 014062, DOI : 10.1088/0031-8949/T167/1/014062

[41] T. Wauters et al, Plasma Phys. Control. Fusion 62 (2020) 034002, DOI: 10.1088/1361-6587/ab5ad0

[42] J.-S. Park et al, Nucl. Fusion 63 (2023) 076027, DOI: 10.1088/1741-4326/acd9d9

[43] J. Gaspar et al, Int. J. Therm. Sci. 104 (2016) 292, DOI: 10.1016/j.ijthermalsci.2016.01.022

[44] J. Romazanov et al, Nucl. Mater. Energy 18 (2019) 331, DOI: 10.1016/j.nme.2019.01.015

[45] J.D. Elder et al, Nucl. Mater. Energy 12 (2017) 755, DOI: 10.1016/j.nme.2017.03.039

[46] D. Matveev et al, Nucl. Instrum. Methods Phys. Res. B 430 (2018) 23, DOI: 10.1016/j.nimb.2018.05.037

[47] T. Wauters et al, PSI-25 conference, June 13-17, 2022, Korea (virtual)